Recent changes in extreme wave events in the Southwestern South Atlantic

Carolina B. Gramcianinov[1], Joanna Staneva[1], Celia R. G. Souza[2,3], Priscila Linhares[3], Ricardo de Camargo[4], and Pedro L. da Silva Dias[4]

[1]Institute for Coastal Systems Analysis and Modeling, Helmholtz-Zentrum Hereon, Max-Planck-Strasse 1, 21502 Geesthacht, Germany

[2]Institute of Environmental Research, Secretariat of Infrastructure and Environment of São Paulo State (SIMA/SP), Rua Joaquim Távora 822, 04015-011, São Paulo, SP, Brazil.

[3]Department of Physical Geography, Faculty of Philosophy, Literature and Human Sciences, University of São Paulo (FFLCH/USP), Av. Prof. Lineu Prestes, 338, 05508-000, São Paulo-SP, Brazil

[4]Department of Atmospheric Sciences, Institute of Astronomy, Geophysics and Atmospheric Science, University of São Paulo, Rua do Matão, 1226, 05508-090, São Paulo-SP, Brazil

Correspondence: C. B. Gramcianinov (carolina.gramcianinov@hereon.de)

Abstract. Over the past decades, the South Atlantic Ocean has experienced several changes, including a reported increase in coastal erosion and floods. This study aims to investigate the recent changes in the extreme wave events over the Southwest South Atlantic (SWSA) – which hosts the most economically important harbours in South America, high oil and gas production demands, and rich biodiversity. This investigation considers not only the occurrence of wave extreme events but also other

5   extreme wave indicators that may impact the off-shore and coastal areas. For a more direct application to future risk assessment and management, we perform a more focused analysis considering the regional monitoring and warning system division established by the Brazilian Navy. We used a coastal hazards database that covers a portion of the coast to investigate how the trends given by the hindcast may impact the coastal zone. Extreme wave events are obtained using the 95th percentile of significant wave height (Hs) from 1993 to 2021, combining the CMEMS global wave reanalysis and near-real-time products.

10   Annual and seasonal statistics are used to analyse the wave mean and extreme climate patterns and trends in the study region, focusing on Hs, peak period, and wave power. With the analysis, an overview of the wave climate in the study domain is made, including the discussion about seasonal differences. Our findings showed significant changes in the SWSA mainly associated with an increase in mean Hs values, wave period, and consequently, the wave power. Narrowing down to the coast impact, we found an increase in the number of coastal hazards in São Paulo State associated with wave forcing in good agreement with

15   the increase in the number of extreme wave events in the adjacent ocean sector.

Short Summary

We analysed the extreme wave events trends in the Southwest South Atlantic in the last 28 years using a wave hindcast and coastal hazards reports. The results showed important changes in the region mainly associated with an increase in mean sea wave height, wave period and wave power. We also found a rise in the number of coastal hazards associated with wave forcing

20   affecting the São Paulo State, which agrees with the increase in the number of extreme wave events in the adjacent ocean sector.

1 Introduction

In recent years, several extreme events have been reported in the South Atlantic Ocean (e.g., Marcello et al., 2018; Dalagnol et al., 2022), thus reflecting directly on hazards along the coast. One of the regions that is facing relevant changes is the Southwestern South Atlantic (SWSA), with the increase in extreme wave occurrence and storm surges (Souza et al., 2019; Gramcianinov et al., 2022). With high economical relevance, the SWSA region hosts strategic harbours in South America, which is responsible for the transportation of 755 million tons of goods in 2021 (ANTAQ, 2022) and promising oil and gas exploration fields. In addition to that, the region also holds rich biodiversity, including coral reefs and 856 km^2 of mangroves that are crucial for hazard coastal protection, economic activities (e.g., fishery) and the cultural identity of the coastal communities (Pereira-Filho et al., 2021; ICMBio, 2018). The SWSA coastal cities have a dense population, with approximately 100 million people who are extremely vulnerable to coastal erosion and coastal infrastructure damages.

Assessing the extreme waves and wave trends in the SWSA with traditional approaches has proven to be challenging for several reasons. The difficulties remain mostly in the still-limited knowledge and understanding of the local physical processes and climate variabilities. Both the limited accuracy of long-term integrations, and the scarce data availability can grieve even more these analyses. Some recent studies have revealed changes in the wave pattern in the South Atlantic usually addressed to the increase in the extreme waves in the Southern Ocean (SO). In general, most previous global or hemispheric-based studies have reported increases in wave height extremes in the Southern Hemisphere (SH) over the past 41 years, and this increase is expected to continue in the future (Caires and Sterl, 2005; Dobrynin et al., 2012; Lemos et al., 2019). However, when focusing on the SWSA the mean and extreme wave climate trends present a larger uncertainty.

In addition to understanding the significant wave height trends, it is of utmost importance to assess changes in wave event characteristics, such as the mean wave direction and peak period. Silva et al. (2020) showed how the oscillation between the south and east dominant wave energy flux directions has led to changes in the coastal morphodynamics at both the regional and local scales. Some previous works reported wave power changes under the present climate conditions (Odériz et al., 2021) and mean wave direction and period changes in future scenarios (Hemer et al., 2010; Lobeto et al., 2021). These changes directly affect naval and coast risk assessments, which demand special efforts to link the regional and local wave extremes more properly.

Under this background, this section aims to report and investigate the recent extreme wave climate trends in the SWSA, while focusing on wave event characteristics such as events frequency, intensity, duration, and peak period. We examine the seasonal statistics and climatic trends using both traditional (i.e., percentile-based) and storm-based approaches to provide new insights into the regional wave climate changes. To obtain results with more direct application to future risk assessment and management we perform a more focused analysis considering the regional monitoring and warning system, as well as the impact of the recent wave climate changes on the coast.

2 Methods

2.1 Datasets

55 The main dataset used in this work was the Copernicus Marine Service (CMEMS) global hindcast, named WAVERYS (Table 2, Ref. No. 1; Law-Chune et al., 2021) complemented with the CMEMS Global Ocean Waves Analysis Near Real-Time product (GLO-NRT; Table 2, Ref. No. 2) to fulfil the period between 1993 and 2021. WAVERYS is available at a 0.20° horizontal grid as 3-hourly outputs from 1993 to 2020 while the wave analysis has a 1/12° horizontal grid as 3-hourly instantaneous output fields. The GLO-NRT product was interpolated to the 0.20° horizontal grid, so a more consistent analysis can be achieved despite

60 using different sources. Both products are produced by the wave model called the Météo France Wave Model (MFWAM) with the dissipation terms developed by Ardhuin et al. (2010). WAVERYS is forced by surface winds and the sea-ice fraction derived from the ERA5 (5th generation reanalysis from the European Centre for Medium-Range Weather Forecast (ECMWF)) and ocean currents obtained from the ocean reanalysis Global Ocean Reanalysis and Simulation (GLORYS). The GLO-NRT is forced only by a 6-hourly winds analysis from the IFS-ECMWF atmospheric system.

65 An evaluation of WAVERYS for the South American wave climate was made by Crespo et al. (2022). These authors compared the Hs from the WAVERYS, ERA5, and the National Center for Environmental Prediction (NCEP) Wave reanalysis (Chawla et al., 2013) against buoy measurements in three locations along the Brazilian coast and found that WAVERYS presented the highest correlation and the lowest root mean square deviation (RMSD). The ERA5 performance in representing the winds is also relevant once this field dominates the wave generation process. Previous works have shown that ERA5 is

70 able to represent the wind climate, extreme percentiles, and even storm variability (e.g., Belmonte Rivas and Stoffelen, 2019; Gramcianinov et al., 2020a; Crespo et al., 2022).

2.2 Percentile computation

In this work, the percentiles were computed using the empirical distribution of the Hs peaks within a given period, using a 48-h time window to select the peaks, thus allowing us to obtain a more detailed view of individual wave events occurrence.

75 This time window has been widely applied in past studies to guarantee that only one peak per storm is used to construct the Hs distribution (e.g., Caires and Sterl, 2005; Meucci et al., 2020). First, the percentile time series were obtained using the seasonal or annual mean of the 95th percentile computed based on the monthly Hs distribution. The wave event analysis, detailed in the next section, was obtained using the seasonal percentile, i.e., the 95th percentile computed for the months within each season. This approach respects the distribution of each season, particularly when they come to present different wave sources (Goda,

80 2010).

2.3 Trends estimation and testing

Trends are estimated based on Sen's slope estimator (Sen, 1968), which evaluates the magnitude of a time series trend. The significance of Sen's slope is calculated by the Mann-Kendall test (Mann, 1945; Kendall, 1975). Both methods are non-

parametric (distribution-free) procedures and consider the monotonic upward or downward of the time series, thus, being more robust to climate-based analysis (e.g., Wang et al., 2020). However, we use the traditional parametric linear regression analysis allied to the bootstrap method (n = 1000) to obtain the trends errors and trend curves confidence intervals. For this reason, in some cases, the trend is considered significant according to the error (the trend is different from zero in a 95% c.i. in the parametric test), but not significant according to the Mann-Kendall test. In this situation, we considered the Mann-Kendall test as the ground truth.

2.4 Wave events analysis

The wave event statistics were derived following the methods developed by (Weisse and Günther, 2007), in which consecutive points over a specific threshold within a given time series are considered to define extreme wave events. This event-counting process is performed for each grid cell considering its unique severe event threshold (SET), defined herein as the 95th-percentile of Hs value computed for the whole period (1993 - 2021). Notably, there is no widely accepted method for selecting threshold values and values between the 90th and 99th-percentile Hs are often used (Leo et al., 2020; Gramcianinov et al., 2020b). Generally, a high threshold is a good choice when the data sample is sufficiently large and the focus is on the most extreme events. The duration of each event was computed by counting the number of time steps during which the curve is above the SET value while the intensity is equal to the difference between the maximum Hs of the event and the SET at that point. The wave event statistics are presented herein both as time series for the entire domain and as spatial distributions corresponding to each parameter. The same analysis was applied successfully in the Black Sea by Staneva et al. (2022), allowing a better understanding of the extreme wave events' spatial distribution and trends. More details about these methods can be found in Weisse and Günther (2007).

2.5 Wave power calculation

Following Staneva et al. (2022), we also calculated the wave power in the study domain. Wave power or wave energy flux was obtained following the Eq. 1:

$$P = (\frac{\rho g^2}{64 \pi}) Hs^2 Te, \tag{1}$$

where P is the wave energy flux per unit of wave-crest length (kW/m), ρ is water density, g is the acceleration due to gravity, Hs is the significant wave height, and Te is the wave energy period. The Te is directly available in the WAVERYS products (named VTM10) and is defined as the mean wave period obtained by the $Te \equiv Tm_{-1,0} = m_{-1}/m_0$, based on the $-1th$ and $0th$ moment of the wave spectrum.

2.6 Coastal risk assessment

Warnings and risk assessment in this region are supervised by the Center of Hydrography of the Brazilian Navy (CHM, from "Centro de Hidrografia da Marinha"), which is recognised by the World Meteorological Organization (WMO) as the issue

service for the MetArea V. According to the CHM monitoring system, the coastal region of SWSA can be divided into 4
115   subareas (see Fig. 4a). These subareas were used to analyze the wave climate trends in the domain considering the regional
specificities and to facilitate future discussion about risk management. This type of analysis may facilitate the applicability of
the results found here to future monitoring and warning system development and improvement.

We used a historical database of coastal hazards in São Paulo State, within subarea C for further investigation of coastal
impacts. The Baixada Santista Coastal Hazards database (BDe-BS; Table 2, Ref. No. 3) covers the period from 1928 to 2021
120   and is obtained using the hemerographic method (mostly newspapers) and material from social media (mostly videos), showing
coastal impacts caused by strong waves and anomalous high tides (either meteorological or astronomical tides) (Souza et al.,
2019; Linhares et al., 2021). Thus, the definition of coastal hazards is mainly based on the processes as coastal erosion and/or
coastal inundation, this later also being forced by continental flooding (heavy rainfall) in estuarine areas. Therefore, the coastal
hazards registered in the BDe-BS represent events with high intensity since they were brought to the attention of the public due
125   to their significant impact on the beaches, destruction of urban structures, public and private properties, as well as disruption
of city's day-to-day and port activities. More details regarding the database can be found in Souza et al. (2019).

Currently, the BDe-BS initiative is maintained by São Paulo State government through the "Preventive Plan for Coastal
Erosion, Coastal Inundation and Flooding" (adapted from the Portuguese: "Plano Preventivo de Defesa Civil para Erosão
Costeira, Inundações Costeiras e Enchentes/Alagamentos causadas por Eventos Meteorológicos-Oceanográficos Extremos
130   como Ressacas do Mar e Marés Altas"). Despite representing a small portion of the coastal area of the SWSA, the number of
intense/extreme events reaching the São Paulo State coast can be considered representative of most of the coastal extension of
the domain in this study, except for the subarea D (see Fig. 4a). The reason for this extrapolation is mainly the lack of long-term
records in other locations, and, in addition to that, the database covers the central portion of the study region in a region with
high economical importance.

3   Results

3.1   Extreme wave climate characterization

The extreme wave climate in the SWSA is mainly controlled by the storm track due to the strongest winds associated with the
cyclones (e.g., Campos et al., 2018). The main storm track position, between 55°S and 30°S, characterises the wave height
distribution by the Hs gradient towards the south (Fig. 1a,e,i) and restricts the most intense extreme events to the southern
140   portion of the domain (Fig. 1c,g,k). Despite sharing a common extreme wave-generation source, as it is possible to see by
the similar mean wave direction distribution (Fig. 1d,h,l), summer (DJF) and winter (JJA) present distinct wave patterns due
to the southward shift of the storm track in the summertime (Hoskins and Hodges, 2005). Thus, the summer presents smaller
values of Hs - and consequently, 95th percentile Hs values (Fig. 1e) - in the study domain, which reflects in a lower number
of events (Fig. 1f) and weaker events (Fig. 1g) than winter and the whole period. Climatologically, the austral autumn (MAM)
145   presents behaviour closer to the summer pattern while spring (SON) remains the winter pattern. For these reasons we are going
to focus on the analysis of the winter since it heads the top list of extreme wave events in the study domains (e.g., Pianca

et al., 2010) During the winter, the main storm track is in its northernmost position (Hoskins and Hodges, 2005), resulting in more wave events (Fig. 1j) than other seasons. Typically, in winter, the region presents relatively long fetches along the coast (southwest/northeast orientated) associated with cyclones generated at approximately 35°S (Gramcianinov et al., 2021). These

150   fetches can be widely intensified by rear anticyclones on the western side of the cyclone, thus causing this configuration to be widely related to the most severe cases observed in the domain (e.g., da Rocha et al., 2004; Machado et al., 2010; Dragani et al., 2013).

The high number of events in the northern boundary of the domain (Fig. 11b,j) can be associated with the South Atlantic Subtropical High (SASH), which is also a generating system in the study region (Pianca et al., 2010). The SASH influences

155   mostly the wave climate by generating easterly waves towards the central Brazilian, northward from 23°S. However, the wave events in this location are associated with relatively small Hs, as it is possible to see by the local 95th percentile Hs values (Fig. 1a,i) and wave events intensities (Fig. 1c,k). For instance, the 95th-percentile Hs values in the northern portion of the domain do not reach 3.5 m in the winter (Fig. 1i).

3.2   Extreme wave events trends

160   Starting from the basic extreme statistics, the Hs 95th-percentile trends present a sparse and weak signal in the study domain, except for the winter (Fig. 2f). The southern coast presented a significant increase in the 95th-percentile Hs value, which is greater than 2 cm/yr in some locations during the wintertime. When looking at the mean Hs trend, it is possible to see a general increase in this wave parameter along the Brazilian continental shelf, covering the coastal and offshore regions. The magnitude of the mean Hs increase is small (< 0,2cm/year), but significant, in the whole period (Fig. 2b). In the winter, the mean Hs

165   increase is relatively greater (between 0.4 and 0.8 cm/year; Fig. 2g). The differences between the mean and 95th-percentile Hs trends signal are in agreement with the findings of Young and Ribal (2019), who showed that the Hs distribution changes in the last years were skewed to the left with an increase of small waves - which can change the mean without changing the extreme percentiles. The trends in the number of extreme wave events also presented sparse behaviour, however, with significant increases along the Brazilian coast (Fig. 2c,h). The event's increase occurred on most of the coast in the whole-

170   period analysis, while it was confined to some portions of the southern and southeastern coast during the winter (Fig. 2h). It is important to note that the rise in the number of events does not follow the 95th-percentile Hs trends pattern.

Figure 2 also presents the spatial trends of the mean distribution of the wave peak period during the events (Fig. 2d,i). There was a general increase in the peak period in the study domain, confined to the central portion of the coast in the winter (Fig. 2i). An increase in the wave peak period together with the increase in the Hs can lead to important changes in the wave power

175   (Eq. 1). In fact, the wave power presented a small, but significant increase along the coast in the whole period and wintertime (Fig. 2e,j). Following the mean Hs behaviour, the increase in the wave power is larger in the winter than in the whole period - as expected, once wave power is proportional to Hs^2 (Eq. 1). Other extreme event indicators, such as intensity, mean wave direction, and lifetime did not present a robust trend signal, and therefore, are not shown. When comparing the whole-period and wintertime analyses, it is possible to note that the latter presents a greater trend signal given the higher intensity of the wave
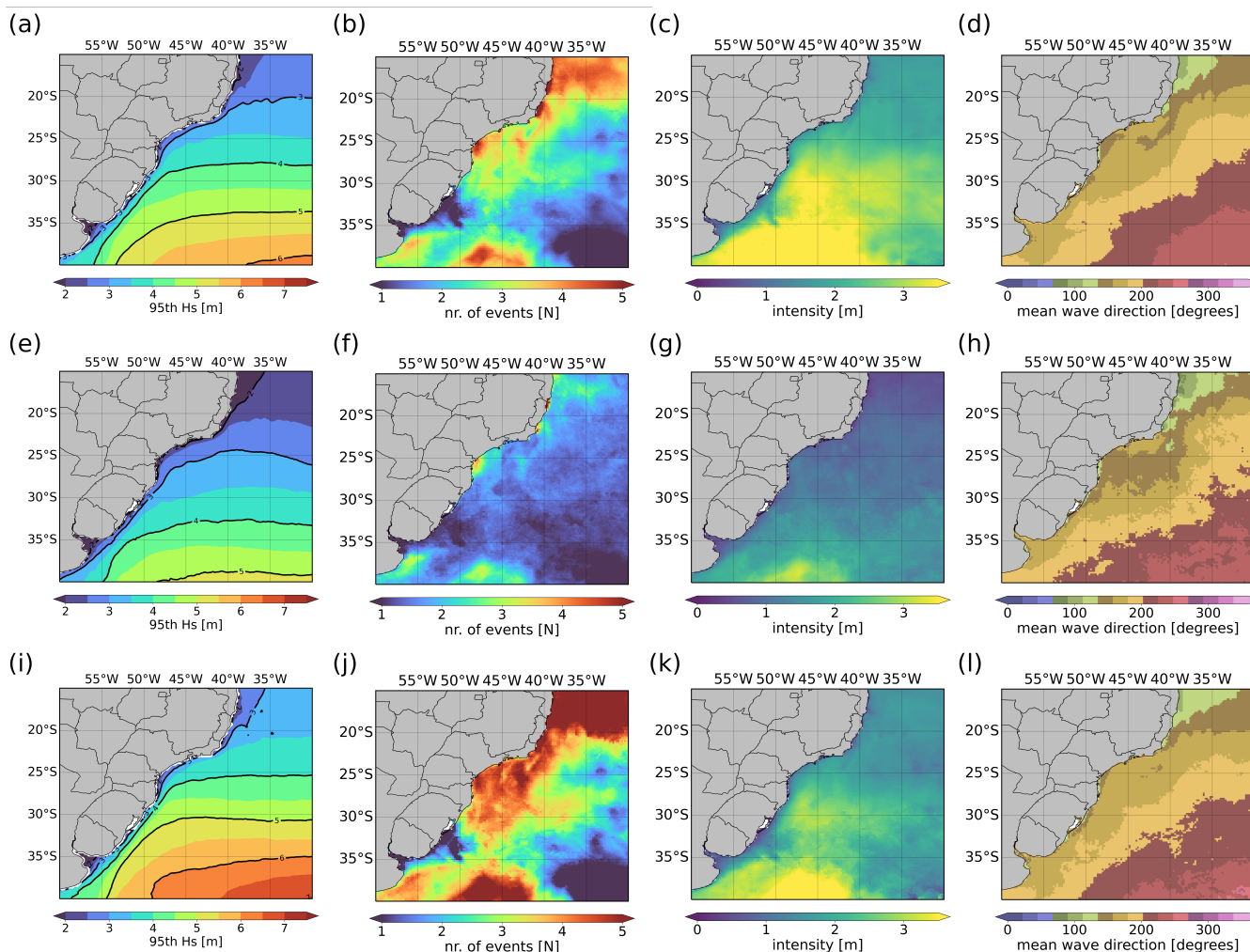
Figure 1. Annual/Seasonal mean (a,e,i) 95th-percentile Hs value (m), extreme wave event (b,f,j) number, (c,g,k) intensity (Hs - 95th Hs) (m) (d,h,l) mean direction (degrees) in the (a-d) whole period (1993-2021), (e-h) summer (DJF), and (i-l) winter (JJA) based on the CMEMS hindcasts (Table 2, Ref. No. 1 and 2)

180   events in this season. Moreover, when considering the trends based on the extreme events, this season presents less variability in the number of events than the whole period analysis, resulting in more robust statistics.

The extreme event analysis based on each grid point in a high-resolution hindcast provides a more detailed view of pattern changes along the coast. On the other hand, such an analysis can produce sparse results that may not be easily applied in more practical and operation tasks. Due to that, the most relevant trends were analysed for each Brazilian Navy's monitoring and

185   warning subareas (Fig. 3). Both C and D subareas present a significant increase in the number of events in the whole period. These regions also presented, together with B, an increase in the mean power wave - despite no significant change in the peak
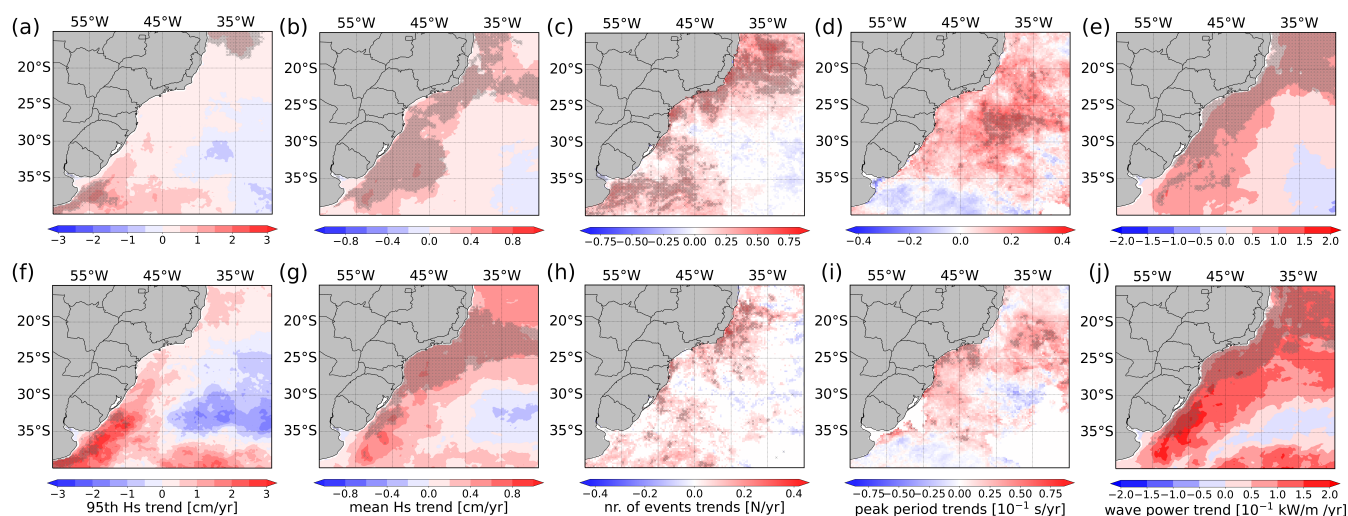
Figure 2. Trends in the (a,f) 95th-percentile and (b,g) mean Hs values (cm/year), extreme wave event (c,h) number (total number / year) and (d,i) peak period (10^{-1} s/year) and (e,j) mean wave power (10^{-1} kW/m / year) in the (a-e) whole period and (f-j) winter (JJA) based on the CMEMS hindcasts (Table 2, Ref. No. 1 and 2). Grey crosses represent points where the trend is significant (Mann-Kendall test; 95% c.i.).

period. In the winter, the A and C subareas presented significant trends in the number of events per year. C subarea presented a small, but significant increase in peak period in the winter, as well as in the wave power. The wave power also increases in subarea D in the winter.

190   By the time series, it is possible to note a high variability as a result of large-scale climate modes that affect the regional wave climate (e.g., Sasaki et al., 2021). However, even considering these variabilities, most of the parameters presented a positive trend, although not always significant. As explained in section 2.3, we consider the Mann-Kendall test to assess the significance of the trends, although the parametric test detects significance in some cases. For instance, the 95th-percentile values presented a significant trend for all subareas according to the parametric test. This also happens in the peak period (only winter) and

195   wave power. The sensitivity of the Mann-Kendall test may be related to the large variance of the time series, which directly influences the trend detected by this method (Wang et al., 2020). Nevertheless, we stand for the robustness of the Mann-Kendall test, especially because most wave parameters, especially in extreme analysis, does not follow a normal distribution required by the parametric test.

3.3   Coastal risk analysis

200   The Charlies subarea (C) is one of the most affected locations, experiencing an increased number of extreme wave events, peak period, and wave power in the last years. However, linking the changes in the regional wave climate with coastal hazards is not a straightforward task once the wave systems are modified by the bathymetry and their impact depends on the coastal morphodynamics. SP coast was affected by 163 hazards between 1993 and 2021, of which 48% (78) were caused exclusively by storm waves and 30% (79) by the combination of waves and tides (either as a result of astronomical or meteorological
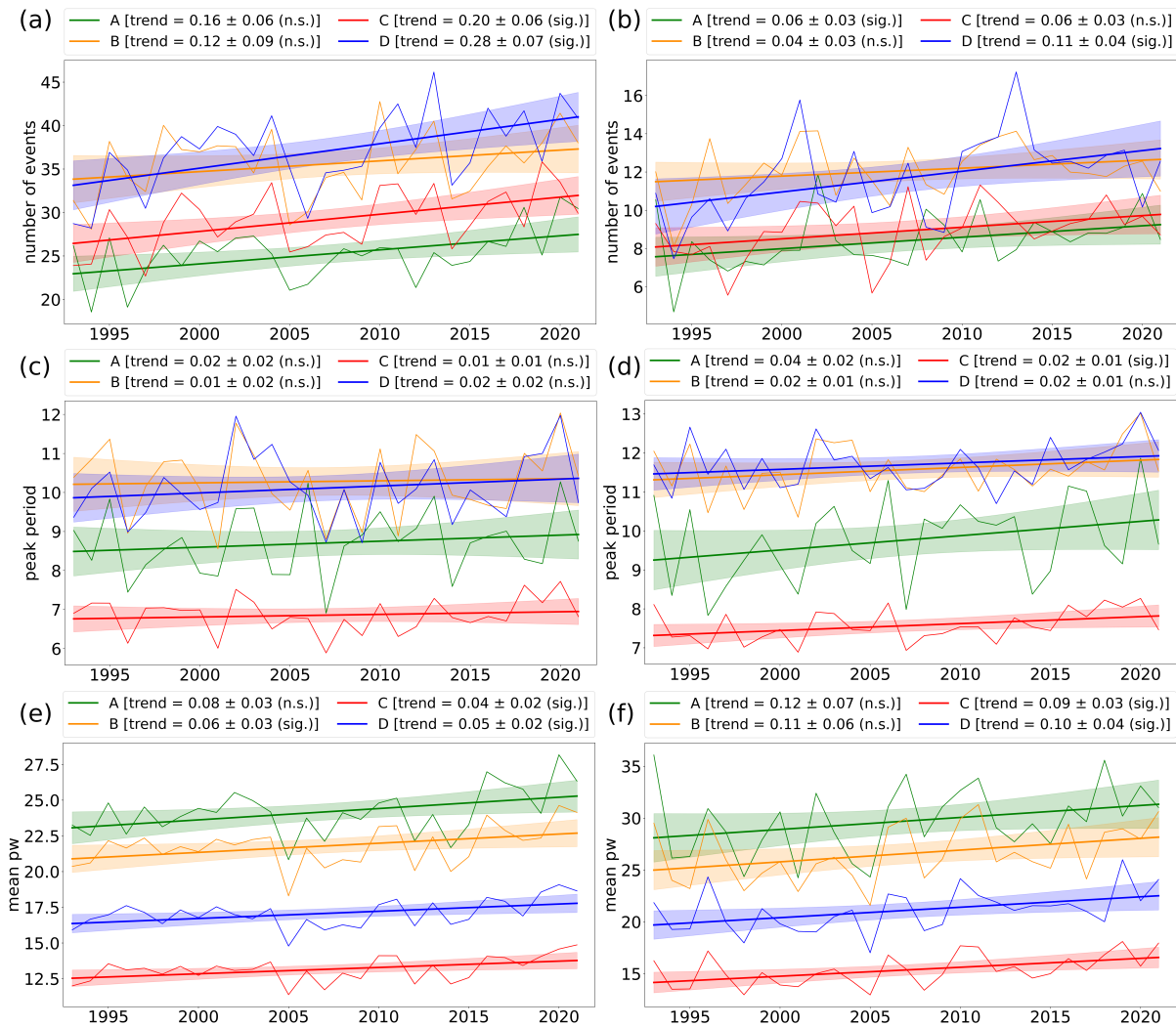
Figure 3. Annual time series and trends in the (a,b) 95th-percentile and (c,d) mean Hs values, extreme wave event (e,f) number and (g,h) peak period, and (i,j) mean wave power in the (a,c,e,g,i) whole period and (b,d,f,h,j) winter (JJA) computed for each Brazilian Navy's warning areas along the study domain's coast based on the CMEMS hindcasts (Table 2, Ref. No. 1 and 2). The trends confidence intervals (shaded) and deviation (in the legend) are computed by bootstrap testing on least square adjustment. N.S. and SIG. in the legend mean not significant and significant, respectively, according to the Mann-Kendall test (95% c.i.).

205   tides). In the winter, 93% (51) of events are associated with waves, with combined events following the same proportion (35%) of total events. Thus, the hazards forced exclusively by tides are rare in the winter, which may be related to the high wave generation in this season. Table 1 presents the number of events, as well as the computed trends for each type of hazard. The number of events on the coast increased both for the whole period and winter (JJA). The increase in the number of coastal hazards was mainly led by wave events since events caused only by tidal influence did not present any significant trend. This

210   increase are in agreement with Souza et al. (2019), who found a pronounced increase in wave-forced hazards after the 2000s
and 2010s decades [226% compared with the 1928-1999 period] when analysed a longer period of the same database (1928 -
2016).

Figure 4 shows the time series of the yearly events of coastal hazards from the BDe-BS against the number of events detected
in the subarea C obtained by the wave event analysis (described in section 2.4). Due to the small number of coastal hazards per

215   year, we show the time series and trends for the whole period to obtain more robust statistics. Nevertheless, the winter trends
presented the same signal and the same relation among the event types as the whole period trends (see Table 1).

Most of the coastal hazards reported by the BDe-BS are associated with waves, either combined or not with a tidal rise.
This is revealed not only by the numbers in Table 1, but also in the time series (Fig. 4b). The trends of all events and events
associated with waves are similar as well, especially considering the trend error. Moreover, it is possible to compare the trends

220   in the coastal hazards forced by waves with the trends of the number of extreme wave events in the C subarea (Fig. 4c; $0.20 \pm$
0.06 events/year in Fig. 3a). Although, there is no total agreement between the extreme events detected in the C subarea and
hazards reported in the coast in the year by year analysis, the trend behaviour is similar. The number of combined events (wave
+ tides) is superposed in Fig. 4c, as well as total events trends. Through these composed pictures, it is possible to see that
differences in the wave-forced coastal hazards and extreme waves events in C subarea may be a result of the influence of sea

225   level rise events. For instance, 2002 and 2009, do not present a peak in the extreme wave events within the C subarea, but they
were marked by a high number of wave-forced coastal hazards related to a higher percentage of combined events. Maybe these
wave events would not become a hazard if the local sea level rises did not allow waves to reach further into the continental
area. The disagreement between the coastal and offshore events time series can be addressed for bathymetry and morphology
reasons. Moreover, coastal hazards can occur also after a sequence of events that result in a more vulnerable coast due to the

230   lack of recovery time (Souza et al., 2019). These parameters are difficult to assess, especially considering the size of the study
domain and are out of the scope of our analysis.

4   Data Availability

The data products used in this article, as well as their names, availability and documentation are summarised in Table 2.

5   Conclusion

235   The present work aimed to assess changes in the extreme wave climate in the SWSA, giving new insights into offshore coastal
risk assessment and management in this domain. Understanding the extreme waves changes is crucial for supporting future
projections, which are indispensable for the design and safety control of ship vessels, offshore and coastal structures and
maintenance (e.g., oil/gas platforms, aquaculture, wind and wave farms), as well as coastal infrastructure (e.g., ports, roads,
and touristic facilities) (e.g., Bitner-Gregersen et al., 2018; Vettor and Guedes Soares, 2020). Our findings showed important

240   changes in the SWSA mainly associated with an increase in the mean Hs values and wave period. These changes have a direct

Table 1. The number of coastal hazards reported by the BDe-BS (Table2, Ref. No. 3) in the whole period (1993 - 2021) and in the winter (JJA). The percentage calculation is based on the total number of events, which represents the sum of events forced only by waves, only by tides (either by astronomical or meteorological components) or by the combination of both ("waves + tides"). The last row highlights all events associated with waves, with or without tidal influence ("waves"). The trends unit is events per year/season and bold values denote significance (Mann-Kendall test; 95% c.i.).

	whole period		winter (JJA)	
	number of events	trend [number/year]	number of events	trend [number/season]
total	163 (100%)	**0.23 ± 0.07**	55 (100%)	**0.14 ± 0.02**
wave + tides	49 (30%)	**0.10 ± 0.03**	19 (35%)	**0.06 ± 0.02**
only waves	78 (48%)	**0.12 ± 0.05**	32 (58%)	**0.06 ± 0.02**
only tides	36 (22%)	0.01 ± 0.03	4 (7%)	0.01 ± 0.01
waves	127 (78%)	**0.22 ± 0.07**	51 (93%)	**0.12 ± 0.02**

Table 2. CMEMS and non-CMEMS products used in this study, including information on data documentation.

Ref. No.	Product name & type	Documentation
1	GLOBAL_MULTIYEAR_WAV_001_032, reanalysis [1993-2020]	QUID: https://catalogue.marine.copernicus.eu/documents/ QUID/CMEMS-GLO-QUID-001-032.pdf PUM: https://catalogue.marine.copernicus.eu/documents/ PUM/CMEMS-GLO-PUM-001-032.pdf
2	GLOBAL_ANALYSIS_FORECAST_WAV_001_027, NRT [2021]	QUID: https://catalogue.marine.copernicus.eu/documents/ QUID/CMEMS-GLO-QUID-001-027.pdf PUM: https://catalogue.marine.copernicus.eu/documents/ PUM/CMEMS-GLO-PUM-001-027.pdf
3	Baixada Santista Coastal Hazards database, hemerographic method [1993-2021]	Souza et al. (2019); Linhares et al. (2021)
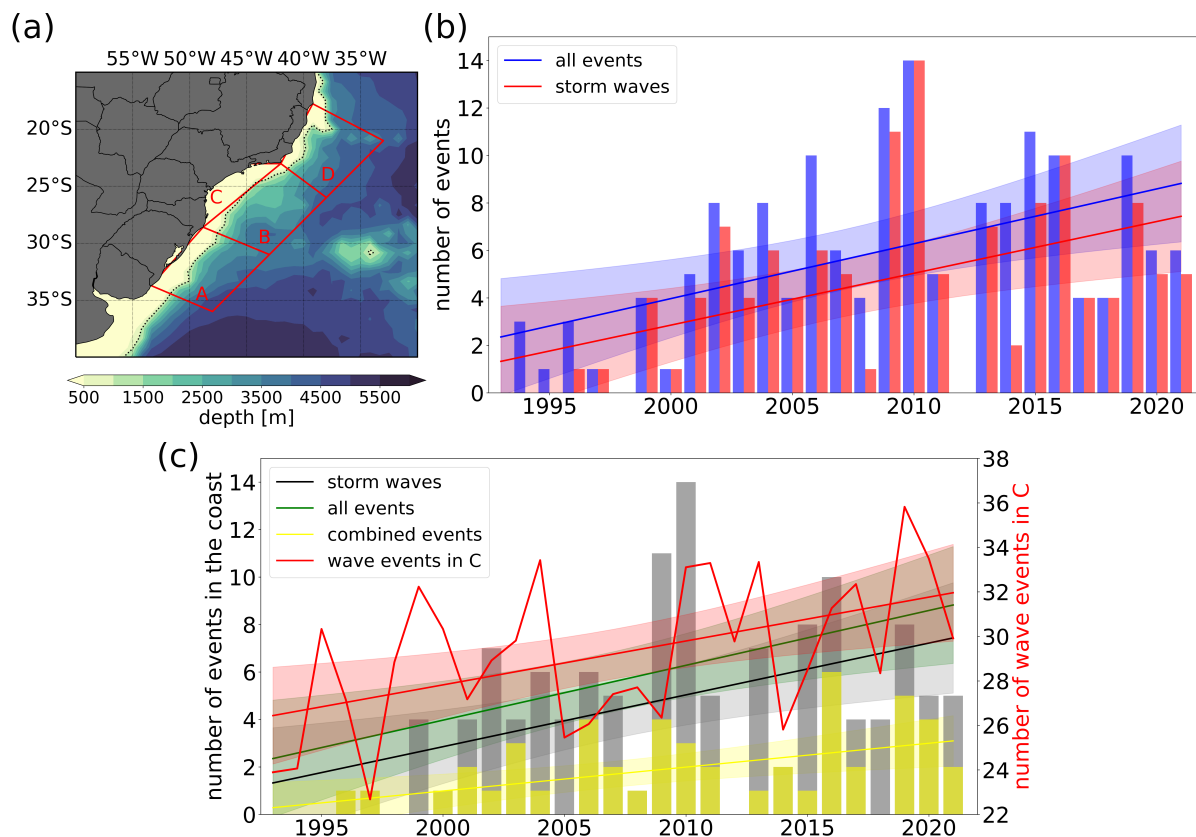
Figure 4. (a) Subareas defined by the Brazilian Navy for warning and monitoring operations; (b) Number of coastal hazards per year caused by any forcing (blue) and waves (red) based on BDe-BS (Table 2, Ref. No. 3); (c) Numbers and trends of coastal hazards per year associated with waves (grey bars and black line) and combined events (waves + tides; yellow bars and lines) based on BDe-BS (Table 2, Ref. No. 3), number and trend of wave events in the subarea C (red lines) based on the CMEMS hindcasts (Table 2, Ref. No. 1 and 2). In panel b and c the 95% c.i. for the trends are shaded in the same colour of each trend.

impact on the offshore and coastal zone, increasing the wave power reaching the region and, consequently, aggravating the coastal hazards along the coast.

Extreme waves are responsible for coastal flooding and coastal erosion (e.g., Machado and Calliari, 2016; Parise et al., 2009), but there still exists a gap between regional and local assessments. Following the Brazilian Navy's monitoring and warning subareas within MetArea V (WMO), most of them require attention regarding wave climate changes. According to WAVERYS hindcast analysis, the number of extreme wave events (above the 95th-percentile Hs) increased in the A, C, and D subareas and the mean wave power increased in the B, C, and D subareas. The trends vary depending on whether the whole period or only wintertime is considered. In this work, we elected winter (JJA) as a representative of a more extreme wave climate, but an extension of the analysis to other seasons is recommended for the future once the Spring (SON) weather

250 patterns are also able to produce severe waves (e.g., Crespo et al., 2022). By our findings, we recommend special attention to C and D subareas once they present changes both in the number of events and wave power.

Regarding the coastal assessment, we found an increase in the number of coastal hazards in São Paulo State. According to our analysis, the increase in coastal hazards in this location is mainly associated with wave forcing and can be related to the increase in the number of extreme wave events in subarea C. Despite the well-known limitation in wave modelling, particularly

255 to extreme waves (e.g., Campos et al., 2018), this finding gives evidence that the WAVERYS hindcast may be useful to assess, not only extreme wave climate in the study domain (as shown by Crespo et al., 2022) but also the events reaching the coast in a long to mid-term perspective. However, for interannual and interseasonal analyses, that require year-by-year assessment, more care is needed, especially because a coastal hazard does not depend only on the waves. Sea level rise, in both climatic and synoptic scales, and astronomical tides play a large role, potentially turning moderate waves into damaged waves once a

260 high sea level allows waves to propagate and break further on in the continent. Souza et al. (2019) highlighted that the most severe coastal hazards reported in the region do not present the highest values of Hs or sea level elevation, but a combination of factors. Many other elements such as coastal vulnerability, precipitation, morphology, and coastline orientation affect the establishment of a coastal hazard (e.g., Souza et al., 2019; Muehe, 2018), particularly when the hazard is defined by its impact on the coast and not by some pure meteorological and/or oceanographic parameter.

265 Therefore, a complete assessment of coastal impacts needs more specific analysis considering local information and data, which is impracticable in this work, considering the study domain size. However, the trends derived herein are a valuable factor in identifying areas that are potentially vulnerable to climate change hazards and are a useful tool for engineers and stakeholders working towards the sustainable development of maritime activities. These changes may require adaptation measures, such as the enhancement of coastal protection (e.g., the building of dikes and harbours' protection measures). The findings reported in

270 this work may also support the designing of new projects and future assessments that will allow the advance of the association of the large-scale wave climate with coastal impacts.

Author contributions. CBG: Conceptualization, Formal analysis, Methodology, Visualization, Writing — original draft. JS: Conceptualization, Methodology, Writing — review & editing, Supervision. CRGS and PLS: Methodology, Writing — review. RC and PLSD: Writing — editing, Supervision.

275 *Competing interests.* The authors declare that they have no conflict of interest.

Acknowledgements. The authors would like to acknowledge Marcel Ricker for his support with the wave event method implementation. The study was supported by the European Green Deal project "Large scale RESToration of COASTal ecosystems through rivers to sea connectivity" (REST-COAST) (grant no. 101037097). We gratefully acknowledge the project DOORS (grant no. 101000518) and DAM Mission project CostalFuture. C.B.G. is funded by the Helmholtz European Partnership 'Research Capacity Building for healthy, produc-

280   tive and resilient Seas' (SEA-ReCap). These study also used data and resources of the projects: "Resposta Morfodinâmica de Praias do Sudeste Brasileiro aos Efeitos da Elevação do Nível do Mar e Eventos Meteorológico-Oceanográficos Extremos até 2100" (CAPES, proc. no. 88887.139056/2017-00), "Sistema de Aviso de Ressacas e Inundações Costeiras para o Litoral de São Paulo, com foco em Impactos das Mudanças Climáticas" (São Paulo Research Foundation (FAPESP), grant 2018/14601-0), and "Extreme wind and wave modelling and statistics in the Atlantic Ocean" (FAPESP, grants #2018/08057-5 and #2020/01416-0).

References

ANTAQ: Anuário da Agência Nacional de Transporttes Aquaviários (ANTAQ), Annual Report of the National Water Transportation Agency, Brazil (in Portuguese), https://anuario.antaq.gov.br, [last access: 12 May 2022], 2022.

Ardhuin, F., Rogers, E., Babanin, A. V., Filipot, J.-F., Magne, R., Roland, A., van der Westhuysen, A., Queffeulou, P., Lefevre, J.-M., Aouf, L., and Collard, F.: Semiempirical Dissipation Source Functions for Ocean Waves. Part I: Definition, Calibration, and Validation, Journal of Physical Oceanography, 40, 1917 – 1941, https://doi.org/10.1175/2010JPO4324.1, 2010.

Belmonte Rivas, M. and Stoffelen, A.: Characterizing ERA-Interim and ERA5 surface wind biases using ASCAT, Ocean Sci., 15, 831–852, https://doi.org/10.5194/os-15-831-2019, 2019.

Bitner-Gregersen, E. M., Vanem, E., Gramstad, O., Hørte, T., Aarnes, O. J., Reistad, M., Breivik, Ø., Magnusson, A. K., and Natvig, B.: Climate change and safe design of ship structures, Ocean Engineering, 149, 226–237, https://doi.org/10.1016/j.oceaneng.2017.12.023, 2018.

Caires, S. and Sterl, A.: 100-year return value estimates for ocean wind speed and significant wave height from the ERA-40 data, J. Clim., 18, 1032–1048, https://doi.org/10.1175/JCLI-3312.1, 2005.

Campos, R. M., Alves, J. H., Guedes Soares, C., Guimaraes, L. G., and Parente, C. E.: Extreme wind-wave modeling and analysis in the South Atlantic ocean, Ocean Model., 124, 75–93, https://doi.org/10.1016/j.ocemod.2018.02.002, 2018.

Chawla, A., Spindler, D. M., and Tolman, H. L.: Validation of a thirty year wave hindcast using the Climate Forecast System Reanalysis winds, Ocean Modelling, 70, 189–206, https://doi.org/https://doi.org/10.1016/j.ocemod.2012.07.005, ocean Surface Waves, 2013.

Crespo, N. M., da Silva, N. P., Palmeira, R. M. d. J., Cardoso, A. A., Kaufmann, C. L. G., Lima, J. A. M., Andrioni, M., de Camargo, R., and da Rocha, R. P.: Western South Atlantic Climate Experiment (WeSACEx): extreme winds and waves over the Southeastern Brazilian sedimentary basins, Clim. Dyn., https://doi.org/10.1007/s00382-022-06340-y, 2022.

da Rocha, R. P., Sugahara, S., and da Silveira, R. B.: Sea Waves Generated by Extratropical Cyclones in the South Atlantic Ocean: Hindcast and Validation against Altimeter Data, Weather and Forecasting, 19, 398–410, https://doi.org/10.1175/1520-0434(2004)019<0398:swgbec>2.0.co;2, 2004.

Dalagnol, R., Gramcianinov, C. B., Crespo, N. M., Luiz, R., Chiquetto, J. B., Marques, M. T. A., Neto, G. D., de Abreu, R. C., Li, S., Lott, F. C., Anderson, L. O., and Sparrow, S.: Extreme rainfall and its impacts in the Brazilian Minas Gerais state in January 2020: Can we blame climate change?, Clim. Resil. Sustain., 1, 1–15, https://doi.org/10.1002/cli2.15, 2022.

Dobrynin, M., Murawsky, J., and Yang, S.: Evolution of the global wind wave climate in CMIP5 experiments, Geophys. Res. Lett., 39, 2–7, https://doi.org/10.1029/2012GL052843, 2012.

Dragani, W. C., Cerne, B. S., Campetella, C. M., Possia, N. E., and Campos, M. I.: Synoptic patterns associated with the highest wind-waves at the mouth of the Río de la Plata estuary, Dyn. Atmos. Ocean., 61-62, 1–13, https://doi.org/10.1016/j.dynatmoce.2013.02.001, 2013.

Goda, Y.: Random Seas and Design of Maritime Structures, WORLD SCIENTIFIC, https://doi.org/10.1142/7425, 2010.

Gramcianinov, C. B., Campos, R. M., de Camargo, R., Hodges, K. I., Guedes Soares, C., and da Silva Dias, P. L.: Analysis of Atlantic extratropical storm tracks characteristics in 41 years of ERA5 and CFSR/CFSv2 databases, Ocean Eng., 216, 108 111, https://doi.org/10.1016/j.oceaneng.2020.108111, 2020a.

Gramcianinov, C. B., Campos, R. M., Guedes Soares, C., and de Camargo, R.: Extreme waves generated by cyclonic winds in the western portion of the South Atlantic Ocean, Ocean Eng., 213, 107 745, https://doi.org/10.1016/j.oceaneng.2020.107745, 2020b.

Gramcianinov, C. B., Campos, R. M., de Camargo, R., and Guedes Soares, C.: Relation between cyclone evolution and fetch associated with extreme wave events in the South Atlantic Ocean, J. Offshore Mech. Arct. Eng., 2A-2020, 1–27, https://doi.org/10.1115/1.4051038, 2021.

Gramcianinov, C. B., de Camargo, R., Campos, R. M., Guedes Soares, C., and da Silva Dias, P.: Impact of Extratropical Cyclone Intensity and Speed on the Extreme Wave Trends in the Atlantic Ocean, Clim. Dyn., pp. 0–34, https://doi.org/https://doi.org/10.21203/rs.3.rs-995499/v1, 2022.

Hemer, M. A., Church, J. A., and Hunter, J. R.: Variability and trends in the directional wave climate of the Southern Hemisphere, Int. J. Climatol., 30, 475–491, https://doi.org/10.1002/joc.1900, 2010.

Hoskins, B. J. and Hodges, K. I.: A New Perspective on Southern Hemisphere Storm Tracks, J. Clim., 18, 4108–4129, https://doi.org/10.1175/JCLI3570.1, 2005.

ICMBio: Atlas dos Manguezais do Brasil, Brazilian Mangrove Atlas (in Portuguese), Instituto Chico Mendes de Conservação da Biodiversidade (ICMBio), Ministério do Meio Ambiente, Brazil, 2018.

Kendall, M.: Rank Correlation Methods. 4th Edition, Charles Griffin, London, 1975.

Law-Chune, S., Aouf, L., Dalphinet, A., Levier, B., Drillet, Y., and Drevillon, M.: WAVERYS: a CMEMS global wave reanalysis during the altimetry period, Ocean Dynamics, 71, 357–378, https://doi.org/10.1007/s10236-020-01433-w, 2021.

Lemos, G., Semedo, A., Dobrynin, M., Behrens, A., Staneva, J., Bidlot, J. R., and Miranda, P. M.: Mid-twenty-first century global wave climate projections: Results from a dynamic CMIP5 based ensemble, Glob. Planet. Change, 172, 69–87, https://doi.org/10.1016/j.gloplacha.2018.09.011, 2019.

Leo, F. D., Solari, S., and Besio, G.: Extreme wave analysis based on atmospheric pattern classification: an application along the Italian coast, Natural Hazards and Earth System Sciences, 20, 1233–1246, https://doi.org/10.5194/nhess-20-1233-2020, 2020.

Linhares, P. S., Fukai, D. T., and Souza, C. R. G.: Clima de ondas e maré em três eventos meteo-oceanográficos extremos ocorridos em São Paulo, em fevereiro e abril de 2020, In: X Congresso sobre Planejamento e Gestão das Zonas Costeiras nos Países de Expressão Portuguesa, APRH/ABRhidro, 06-10/12/2021 (on-line), [Portuguese], 2021.

Lobeto, H., Menendez, M., and Losada, I. J.: Projections of Directional Spectra Help to Unravel the Future Behavior of Wind Waves, Front. Mar. Sci., 8, https://doi.org/10.3389/fmars.2021.655490, 2021.

Machado, A. A. and Calliari, L. J.: Synoptic systems generators of extreme wind in Southern Brazil: atmospheric conditions and consequences in the coastal zone, J. Coast. Res., 1, 1182–1186, https://doi.org/10.2112/SI75-237.1, 2016.

Machado, A. A., Calliari, L. J., Melo, E., and Klein, A. H.: Historical assessment of extreme coastal sea state conditions in southern Brazil and their relation to erosion episodes, Panam. J. Aquat. Sci., 5, 105–114, 2010.

Mann, H. B.: Nonparametric Tests Against Trend, Econometrica, 13, 245–259, http://www.jstor.org/stable/1907187, 1945.

Marcello, F., Wainer, I., and Rodrigues, R. R.: South Atlantic Subtropical Gyre Late Twentieth Century Changes, Journal of Geophysical Research: Oceans, 123, 5194–5209, https://doi.org/10.1029/2018jc013815, 2018.

Meucci, A., Young, I. R., Hemer, M., Kirezci, E., and Ranasinghe, R.: Projected 21st century changes in extreme wind-wave events, Sci. Adv., 6, eaaz7295, https://doi.org/10.1126/sciadv.aaz7295, 2020.

Muehe, D.: Panorama da Erosão Costeira no Brasil, Ministério do Meio Ambiente – MMA (Brazilian Ministry of the Environment), available in http://www.mma.gov.br/publicacoes-mma [in Portuguese], 2018.

Odériz, I., Silva, R., Mortlock, T. R., Mori, N., Shimura, T., Webb, A., Padilla-Hernández, R., and Villers, S.: Natural Variability and Warming Signals in Global Ocean Wave Climates, Geophys. Res. Lett., 48, 1–12, https://doi.org/10.1029/2021GL093622, 2021.

Parise, C., Calliari, L., and Krusche, N.: Extreme storm surges in the south of Brazil: atmospheric conditions and shore erosion, Brazilian Journal of Oceanography, 57, 175–188, 2009.

360 Pereira-Filho, G. H., Mendes, V. R., Perry, C. T., Shintate, G. I., Niz, W. C., Sawakuchi, A. O., Bastos, A. C., Giannini, P. C. F., Motta, F. S., Millo, C., Paula-Santos, G. M., and Moura, R. L.: Growing at the limit: Reef growth sensitivity to climate and oceanographic changes in the South Western Atlantic, Global and Planetary Change, 201, 103 479, https://doi.org/10.1016/j.gloplacha.2021.103479, 2021.

Pianca, C., Mazzini, P. L. F., and Siegle, E.: Brazilian offshore wave climate based on NWW3 reanalysis, Brazilian J. Oceanogr., 58, 53–70, 2010.

365 Sasaki, D. K., Gramcianinov, C. B., Castro, B., and Dottori, M.: Intraseasonal variability of ocean surface wind waves in the western South Atlantic: the role of cyclones and the Pacific South American pattern, Weather Clim. Dyn., 2, 1149–1166, https://doi.org/10.5194/wcd-2-1149-2021, 2021.

Sen, P. K.: Estimates of the Regression Coefficient Based on Kendall's Tau, Journal of the American Statistical Association, 63, 1379–1389, https://doi.org/10.1080/01621459.1968.10480934, 1968.

370 Silva, A. P., Klein, A. H., Fetter-Filho, A. F., Hein, C. J., Méndez, F. J., Broggio, M. F., and Dalinghaus, C.: Climate-induced variability in South Atlantic wave direction over the past three millennia, Sci. Rep., 10, 1–12, https://doi.org/10.1038/s41598-020-75265-5, 2020.

Souza, C. R. d. G., Souza, A. P., and Harari, J.: Long Term Analysis of Meteorological-Oceanographic Extreme Events for the Baixada Santista Region, in: Climate Change in Santos Brazil: Projections, Impacts and Adaptation Options, pp. 97–134, Springer International Publishing, https://doi.org/10.1007/978-3-319-96535-2_6, 2019.

375 Staneva, J., Ricker, M., Akpınar, A., Behrens, A., Giesen, R., and von Schuckmann, K.: Long-term interannual changes in extreme winds and waves in the Black Sea, Copernicus Marine Service Ocean State Report 2021 (issue 6), [accepted], 2022.

Vettor, R. and Guedes Soares, C.: A global view on bimodal wave spectra and crossing seas from ERA-interim, Ocean Engineering, 210, 107 439, https://doi.org/10.1016/j.oceaneng.2020.107439, 2020.

Wang, F., Shao, W., Yu, H., Kan, G., He, X., Zhang, D., Ren, M., and Wang, G.: Re-evaluation of the Power of the Mann-Kendall Test for
380 Detecting Monotonic Trends in Hydrometeorological Time Series, Frontiers in Earth Science, 8, https://doi.org/10.3389/feart.2020.00014, 2020.

Weisse, R. and Günther, H.: Wave climate and long-term changes for the Southern North Sea obtained from a high-resolution hindcast 1958–2002, Ocean Dyn., 57, 161–172, https://doi.org/10.1007/s10236-006-0094-x, 2007.

Young, I. R. and Ribal, A.: Multiplatform evaluation of global trends in wind speed and wave height, Science (80-.)., 364, 548–552,
385 https://doi.org/10.1126/science.aav9527, 2019.